Title: A Nonhuman Primate Model of Liver Fibrosis towards Cell Therapy for Liver Cirrhosis

Authors: Katsutaro Yasuda [a, b], Maki Kotaka [a], Takafumi Toyohara [a], Shin-Ichi Sueta [a], Yuko Katakai [c], Naohide Ageyama [d], Shinji Uemoto [b], Kenji Osafune [a, *]

[a] *Center for iPS Cell Research and Application* (*CiRA*), *Kyoto University, 53 Shogoin Kawahara-cho, Sakyo-ku, Kyoto, 606-8507, Japan*.

[b] *Department of Hepatobiliary Pancreatic Surgery and Transplantation, Graduate School of Medicine, Kyoto University, 54 Shogoin Kawahara-cho, Sakyo-ku, Kyoto, 606-8507, Japan*.

[c] *The Corporation for Production and Research of Laboratory Primates, Sakura 1-16-2, Tsukuba, Ibaraki, 305-0003, Japan*.

[d] *Tsukuba Primate Research Center, National Institutes of Biomedical Innovation, Health and Nutrition* (*NIBIOHN*), *Hachimandai 1-1, Tsukuba, Ibaraki, 305-0843, Japan*.

* Corresponding author. Center for iPS Cell Research and Application (CiRA), Kyoto University, 53 Shogoin Kawahara-cho, Sakyo-ku, Kyoto, 606-8507, Japan.

Tel: 81-75-366-7058; Fax: 81-75-366-7077; Email: osafu@cira.kyoto-u.ac.jp (K. Osafune).

Abstract:

Orthotopic liver transplantation (OLT) is the only curative treatment for refractory chronic liver failure in liver cirrhosis. However, the supply of donated livers does not meet the demand for OLT due to donor organ shortage. Cell therapy using hepatocyte-like cells derived from human induced pluripotent stem cells (hiPSC-HLCs) is expected to mitigate the severity of liver failure, postpone OLT and ameliorate the insufficient liver supply. For the successful clinical translation of hiPSC-based cell therapy against liver cirrhosis, realistic animal models are required. In this study, we created a nonhuman primate (NHP) liver fibrosis model by repeated administrations of thioacetamide (TAA) and evaluated the short-term engraftment of hiPSC-HLCs in the fibrotic liver. The NHP liver fibrosis model reproduced well the pathophysiology of human liver cirrhosis including portal hypertension. Under immunosuppressive treatment, we transplanted *ALBUMIN-GFP* reporter hiPSC-HLC aggregates into the fibrotic livers of the NHP model via the portal vein. Fourteen days after the transplantation, GFP-expressing hiPSC-HLC clusters were detected in the portal areas of the fibrotic livers. These results will facilitate preclinical studies using the NHP liver fibrosis model and help establish iPSC-based cell therapies against liver cirrhosis.

Keywords: Liver cirrhosis; NHP model; iPSC; Cell therapy

Abbreviations: ceMRI, contrast-enhanced magnetic resonance imaging; HA, hyaluronic acid; hiPSC, human induced pluripotent stem cell; HLC, hepatocyte-like cell; HT, hepatocyte transplantation; ICG-R15, indocyanine green retention rate at 15 minutes after intravenous injection; NHP, nonhuman primate; OLT, orthotopic liver transplantation; TAA, thioacetamide.

Funding:

This study was supported by the Japan Agency for Medical Research and Development (AMED) through its research grant "Core Center for iPS Cell Research, Research Center Network for Realization of Regenerative Medicine".

Conflict of interest:

Kenji Osafune is a founder and member without salary of the scientific advisory boards of iPS Portal Japan.

Main Text

1. Introduction

Orthotopic liver transplantation (OLT) offers a definitive treatment for patients with refractory chronic liver failure in liver cirrhosis. However, the shortage of donor livers leaves many patients on waiting lists for the operation, with a significant proportion dying every year

[1,2]. Hepatocyte transplantation (HT) using fresh or cryopreserved hepatocytes procured from donor livers is expected to help reduce the problem of donor organ shortage [3]. However, although the results of preclinical HT studies using rodent models are promising [4-5], clinical outcomes are variable [6]. One reason for these discrepancies is a severe shortage of donor livers. Because OLT is the definitive treatment for fatal liver failure, transplantable donor livers are preferentially provided for OLT [7,8]. However, the shortage of proper quality donor livers limits the number and scale of clinical studies of HT and disturbs their outcomes [7,8]. Another reason for the discrepancies includes species differences between humans and rodents. Studies of human biology using rodent models have limitations due to differences in technical aspects and the genetic diversity of humans [9].

Human induced pluripotent stem cells (hiPSCs), which have the ability to proliferate indefinitely and the capability to differentiate into hepatocyte-like cells (hiPSC-HLCs), are expected to be a promising alternative cell source for HT [10-11]. Several reports have already demonstrated the efficacy of iPSC-based cell therapy against fatal liver injury in model mice [11], but different animal models using animals allied to humans are required to evaluate the feasibility of iPSC-based cell therapies. Because of their physiological and anatomical similarity to humans, nonhuman primate (NHP) models have already served in various translational researches on pluripotent stem cell-based cell therapies [12,13]. Further, several NHP liver fibrosis models have been reported [14-16], but not for HT. To assess the efficacy

of cell therapies using hiPSC-HLCs, NHP models which develop severe liver fibrosis and allow hiPSC-HLCs to engraft in the livers are required.

In the current study, we created such an NHP model of severe liver fibrosis using *Macaca fascicularis* with a simple drug-induction method. Subsequently, under immunosuppressive treatment, we transplanted hiPSC-HLCs into the fibrotic livers of the model via the portal vein in the manner used in clinical HT and evaluated their short-term engraftment.

2. Materials and methods

2.1. Animals

All animal experiment procedures were approved by the CiRA Animal Experiment Committee and the animal welfare and animal care committee of the National Institutes of Biomedical Innovation, Health and Nutrition (NIBIOHN, Osaka, Japan). All the macaques were bred and maintained at the Tsukuba Primate Research Center (Ibaraki, Japan). All experimental and animal care procedures were carried out in accordance with the guidelines of the Tsukuba Primate Research Center and the Primate Society of Japan, and the Institute for Laboratory Animal Research (ILAR) guide for care and use of laboratory animals (National Research Council. 2011. Guide for the care and use of laboratory animals: eighth edition. Washington, DC: National Academies Press.).

2.2. Liver fibrosis induction

We adopted thioacetamide (TAA) as a hepatotoxin to induce liver fibrosis [17]. TAA (Fujifilm Wako, cat. no. 204-00881) was administered to macaques by subcutaneous injections twice a week. The dosage of TAA was between 60 to 240 mg/kg body weight/week and adjusted based on the conditions of the macaques.

2.3. Blood sample analysis

Blood sampling was performed under general anesthesia by the intramuscular injection of 10 mg/kg body weight ketamine hydrochloride (Ketalar for intramuscular injection, Daiichi-Sankyo Propharma). All blood sample analyses except for plasma ammonia concentrations were performed by Kotobiken Medical Laboratories (Ibaraki, Japan). The analysis of plasma ammonia concentrations was performed on a DRI-CHEM 3030 (Fujifilm) using FUJI DRI-CHEM SLIDE NH3-PII (Fujifilm) at the Tsukuba Primate Research Center. The indocyanine green (ICG) retention test was carried out according to the manufacturer's protocol. Briefly, ICG (Diagnogreen, Daiichi-Sankyo Propharma) was dissolved in 5 mg/ml with distilled water, and 0.1 ml/kg body weight ICG solution was injected into one saphenous vein. Before the ICG injection, blood sampling was conducted for the blank sample. Fifteen minutes after the ICG injection, blood sampling was performed from the other saphenous vein,

and the plasma ICG concentration was measured at Kotobiken Medical Laboratories. The decreasing rate of plasma ICG concentration (ICG-R15) reflects hepatic reserve.

2.4. Liver biopsy

Anesthesia was induced by the intramuscular injection of 10 mg/kg body weight ketamine hydrochloride and 0.5 mg/kg body weight xylazine hydrochloride (Seraktar (also called Rompun), Bayer), and maintained by mask anesthesia with 2% inhaled isoflurane (Isoflurane inhalation solution, Pfizer). After the laparotomy, the edge of the liver was cut with a scalpel, and the obtained liver blocks were fixed with 10% (vol/vol) formalin neutral buffer solution (Fujifilm Wako, cat. no. 062-01661). From days 0 to 2 after the liver biopsy, 50 mg/kg body weight/day cefazolin sodium hydrate (Cefamezin alpha, Astellas Pharma) was intramuscularly administered to prevent infection, and 0.02 mg/kg body weight/day buprenorphine hydrochloride (Zalban, Nissin Pharmaceutical) was intramuscularly administered as an analgesic. Liver fibrosis was assessed by Azan staining and Masson's trichrome staining of the paraffin-embedded liver biopsy specimens. The sections were observed and analyzed using an OLYMPUS BX51 microscope (Olympus) and ImageJ software (National Institutes of Health, Bethesda, Maryland, USA).

2.5. MR imaging

When the macaques underwent euthanasia 14 days after the cell transplantation, contrast-enhanced magnetic resonance imaging (ceMRI) was performed under deep anesthetized condition achieved by an overdose intravenous injection of pentobarbital sodium (Somnopentyl, Kyoritsu Seiyaku) after anesthetic induction by the intramuscular injection of 10 mg/kg body weight ketamine hydrochloride. The ceMRI was performed with a 3T MR scanner (Magnetom Allegra, Siemens). The MRI contrast agent used was gadopentetate dimeglumine (Magnevist, Bayer).

2.6. Cell lines

Experiments using hiPSCs were approved by the ethics committees of Kyoto University and NIBIOHN. In this study, we used the *ALBUMIN-GFP* reporter hiPSC line, which was established in our laboratory [18]. HepG2, a human hepatoma cell line, was obtained from American Type Culture Collection (ATCC).

2.7. Cell culture and hepatic differentiation

Undifferentiated hiPSCs were maintained under on-feeder culture conditions. Hepatic differentiation was performed in accordance with a modified version of previously reported protocols [18]. For more information, refer to the supplementary material.

2.8. Cell transplantation

The Groshong NXT ClearVue 4Fr Single-Lumen Catheter, Basic Tray with Safety Introducer (BD, cat. no. 7617405) containing a 14-gauge vessel catheter sheath and 4 Fr single lumen catheter was used for the hiPSC-HLC transplant. After laparotomy under general anesthesia like liver biopsy, the vessel catheter sheath was indwelled into the drainage vein of the descending colon, and the 4 Fr catheter was advanced into the anterior segment of the right hepatic lobe via the sheath through the portal vein. Iohexol (Omnipaque, Daiichi-Sankyo Propharma) was used as radiopaque contrast media in the portal venography. Then, 1.0×10^3 hiPSC-HLC aggregates were intensively delivered into the segment through the catheter. Immunosuppression for the xenotransplantation was achieved by the administration of a cocktail of three drugs [19]. Daily intramuscular tacrolimus (Prograf, Astellas Pharma) injection was started 5 days before the transplantation. We confirmed whole blood concentrations of tacrolimus on days 0, 7 and 14. The dosage of tacrolimus injection was started at 0.05 mg/kg/day and properly adjusted for the whole blood tacrolimus concentration to be within 5-15 ng/ml. Methylprednisolone was intravenously administered at 500 mg (Sawai Pharmaceutical) on day 0 before the transplantation and intramuscularly at 1 mg/kg (Depo-Medrol, Pfizer) every day after the transplantation until euthanasia. Abatacept (Orencia, Ono Pharmaceutical) was intravenously administered at 12.5 mg/kg on day 0 during the operation. Infection prevention and pain management were carried out like liver biopsy.

2.9. Immunostaining

hiPSC-HLC aggregates were fixed with 4% (wt/vol) paraformaldehyde (PFA) (Nacalai Tesque, cat. no. 26126-54)/PBS (Nacalai Tesque, cat. no. 14249-24). After soaking in 30% sucrose (Nacalai Tesque, cat. no. 30406-25)/PBS, the aggregates were embedded in Tissue-Tek O.C.T. Compound (Sakura Finetek, cat. no. 4583) and frozen. The frozen blocks were sliced into 6- to 10-μm-thick sections.

After euthanasia, the livers of the macaques were removed, immediately cut into slices and immersed into 10% (vol/vol) formalin neutral buffer solution (Fujifilm Wako, cat. no. 062-01661). After soaking in 30% sucrose/PBS, the tissue slices were cut to moderate size, embedded in Tissue-Tek O.C.T. Compound and frozen. The frozen blocks were sliced into 6- to 10-μm-thick sections, and antigen retrieval with HistoVT One (Nacalai Tesque, cat. no. 06380-05) was additionally performed.

Immunohistochemical analyses were carried out after blocking with DS-PBT buffer containing 5% (vol/vol) donkey serum (Merck, cat. no. S30-100ML) and 0.4% (vol/vol) Triton X-100 (Nacalai Tesque, cat. no. 35501-15) in PBS. The primary antibodies used in this study are detailed in Supplementary Table 3. Alexa Fluor conjugated secondary antibodies (Thermo Fisher Scientific) were used for the fluorescence detection. Nuclei were counterstained with 10 μg/ml Hoechst 33342 (Thermo Fisher Scientific, cat. no. H3570). The sections were observed

and analyzed using a BZ-X710 fluorescence microscope (Keyence) and ImageJ software.

2.10. Immunohistochemistry for GFP followed by Masson's trichrome staining

Paraffin-embedded liver tissue blocks were sectioned at 3-μm thickness. After deparaffinization, antigen retrieval was carried out by microwave heating in 0.01 M citrate buffer (pH 6.0). Endogenous peroxidase activity was blocked by 0.3% (vol/vol) hydrogen peroxide (Fujifilm Wako, cat. no. 081-04215) in methanol (Fujifilm Wako, cat. no. 137-01823). After blocking with 1% bovine serum albumin (BSA) (MP Biomedicals, cat. no. 103700)/PBS, anti-GFP antibody (Supplementary Table 3) was applied to the slides. DAB staining was carried out by using a VECTASTAIN Elite ABC Standard Kit (Vector Laboratories, cat. no. PK-6100), biotinylated goat anti-rabbit IgG antibody (Vector Laboratories, cat. no. BA-1000, lot no. X0524) and DAB (Dojindo, cat. no. 349-00903). Subsequently, Masson's trichrome staining was performed. The sections were observed and analyzed using the OLYMPUS BX51 microscope and ImageJ software.

2.11. Statistical analysis

All statistical analyses were performed using GraphPad PRISM 7 (GraphPad Software Inc.).

3. Results

3.1. Induction of liver fibrosis in macaques

Six macaques (*Macaca fascicularis*) were used in this study (Table 1). The experimental design is illustrated in Fig. 1A. Because the proper dosage and administration period of TAA for the creation of liver fibrosis varies among macaques [16], we identified the appropriate conditions for each macaque in the 1st induction stage. These conditions were applied to each macaque in the 2nd induction stage. The liver fibrosis generation was properly assessed by the histology of the liver biopsies.

Just after the TAA administration was started, the serum levels of alanine aminotransferase (ALT) increased like in acute hepatitis (Fig. 1B). However, despite the continuation of TAA administration, ALT levels immediately decreased to approximately normal range. In contrast, the serum concentrations of iron were high throughout the 1st and 2nd induction stages (Fig. 1C). The serum concentrations of gamma glutamyl transpeptidase (γGTP) were also high in the induction stages, although the change was not statistically significant (Supplementary Fig. 1). The long-term administration of TAA resulted in thrombocytopenia (Fig. 1D) and a decrease in albumin synthesis ability (Fig. 1E). Hepatic reserve also decreased after each induction stage (Fig. 1F). However, we could not find any significant changes in blood coagulation (Fig. 1G), ammonia clearance (Fig. 1H) or serum bilirubin concentrations (Fig. 1I).

3.2. Histological assessment of liver fibrosis in the NHP model

Liver biopsies were conducted to assess the effects of long-term TAA administration (Fig. 2A and B). Liver fibrosis was evaluated with the Ishak fibrosis score (Fig. 2C, Supplementary Table 1) [20]. After the 1st induction stage, histological examination revealed marked centrilobular necrosis. Interestingly, centrilobular and portal fibrosis progressed for 3 months after the withdrawal of TAA. On the other hand, hepatic function, such as albumin production, gradually recovered after the withdrawal of TAA (Fig. 2D). Serum hyaluronic acid (HA) levels, a marker of matrix metabolism [21], were significantly higher just after the 1st induction stage and tended to remain so for at least 3 months after the withdrawal (Fig. 2E). After 6 months or longer, liver fibrosis gradually improved. However, at 12 months, liver histology did not recover completely, and portal fibrosis still existed (Fig. 2F and G). After the 2nd induction stage, the development of bridging fibrosis and the formation of regenerative nodules, which indicate liver cirrhosis, were observed (Fig. 2A and C).

3.3. Anatomical features of human liver cirrhosis in the NHP model

After euthanasia, the macaques underwent dissection. The livers of the macaques with fibrosis were atrophic and had uneven surfaces. In particular, atrophy of the right lobe, a typical finding of cirrhosis, was outstanding (Fig. 3A) [2]. The macaques with liver fibrosis had

enlarged spleens (Fig. 3B and C) and dilated portal veins (Fig. 3D-F), indicating portal hypertension. No macaques with liver fibrosis displayed ascites, varices or encephalopathy. Taken together, we succeeded in developing an NHP liver fibrosis model that mimics the pathological features of human liver cirrhosis.

3.4. Transplant of ALBUMIN-GFP reporter hiPSC-HLCs in macaque livers

Subsequently, we transplanted hiPSC-HLCs into the livers of the NHP model and of normal macaques. The experimental design of the transplantation assay is represented in Fig. 4A. Ten days after the 2nd induction stage, the hiPSC-HLC aggregates were transplanted into the fibrotic livers of macaques #1, #2 and #3 and the normal livers of macaques #4 and #5. The dosage of tacrolimus (Supplementary Table 2) was controlled according to its whole blood concentration (see Materials and Methods; Fig. 4B). To trace the hiPSC-HLCs in the livers, *ALBUMIN* (*ALB*)-*GFP* reporter hiPSCs established in our laboratory were used (Fig. 4C and D) [18]. To easily detect the engraftment of the hiPSC-HLCs by immunohistochemistry, the hiPSC-HLC aggregates were locally delivered into the anterior segment of the liver via the portal vein with a vessel catheter (see Materials and Methods; Fig. 4E and F).

Because transplantation procedures with cell dissociation may cause serious damage to hiPSC-HLCs and lower the engraftment efficiency, the cell aggregate culture technique was applied to previously reported differentiation protocols (see Materials and Methods;

Supplementary Fig. 2A). Immunostaining and reverse transcription-polymerase chain reaction (RT-PCR) analyses showed that the hiPSC-HLC aggregates were mainly composed of human ALBUMIN (hALB)-positive hepatic lineage cells (Supplementary Fig. 2B and C). Additionally, the hiPSC-HLC aggregates had albumin synthesis and secretion ability (Supplementary Fig. 2D).

All the macaques that received the hiPSC-HLC transplant were euthanized and dissected 14 days after the transplant. Immunohistochemistry revealed that clusters of GFP- and hALB-double-positive hiPSC-HLCs lay scattered and survived in the expanded portal areas of the fibrotic livers of macaques #1, #2 and #3 (Fig. 4G-I). There were no engraftments of hiPSC-HLCs in the normal livers of macaques #4 and #5 even though tacrolimus concentrations in the normal macaques were not significantly lower than those in fibrosis macaques (Fig. 4J and K). Images of immunohistochemistry for GFP followed by Masson's trichrome staining of the fibrotic livers of the recipients clearly showed that the engrafted GFP-expressing hiPSC-HLCs located not inside the interlobular veins but in the interlobular connective tissue around the vessels of the portal areas (Fig. 4L-N).

4. Discussion

Scarce donor livers are preferentially used for OLT, and the small number of HT cases has made it difficult to correctly evaluate the therapeutic effect on liver diseases [7,8].

Regarding inherited metabolic liver diseases with architecturally normal livers, there have been several preclinical studies using macaques with normal livers, and promising clinical studies are emerging [22]. On the contrary, regarding liver failure resulting from liver cirrhosis, proper NHP models for HT are lacking. Altogether, to progress towards the clinical application of HT for liver failure, the procurement of alternative cell sources and the establishment of proper NHP models are necessary.

In liver cirrhosis, hepatic architectural abnormalities hamper the engraftment of transplanted hepatocytes into the liver [7,8]. Our NHP liver fibrosis model reproduced deranged hepatic architectures like liver cirrhosis. Furthermore, hiPSC-HLCs could engraft in the cirrhotic livers of the model, although longer observation and functional assessment of the transplanted hiPSC-HLCs are still required.

In summary, we have created an NHP liver fibrosis model which reproduces human liver cirrhosis well and allows hiPSC-HLCs to engraft in the livers. This study should provide new insights toward a large-scale preclinical study using NHP liver fibrosis models and contribute to the establishment of iPSC-based cell therapies against liver cirrhosis.

Acknowledgements:

The authors thank Dr. Peter Karagiannis, CiRA, Kyoto University, for critically reading and revising the manuscript, and the Center for Anatomical, Pathological and Forensic

Medical Research, Kyoto University Graduate School of Medicine, for preparing the microscope slides.

References

[1] S.K. Asrani, H. Devarbhavi, J. Eaton, P.S. Kamath, Burden of liver diseases in the world, J Hepatol 70 (2019) 151-171.

[2] D. Schuppan, N.H. Afdhal, Liver cirrhosis, Lancet 371 (2008) 838-851.

[3] S.C. Strom, R.A. Fisher, M.T. Thompson, A.J. Sanyal, P.E. Cole, J.M. Ham, M.P. Posner, Hepatocyte transplantation as a bridge to orthotopic liver transplantation in terminal liver failure, Transplantation 63 (1997) 559-569.

[4] N. Kobayashi, M. Ito, J. Nakamura, J. Cai, C. Gao, J.M. Hammel, I.J. Fox, Hepatocyte transplantation in rats with decompensated cirrhosis, Hepatology 31 (2000) 851-857.

[5] H. Nagata, M. Ito, J. Cai, A.S. Edge, J.L. Platt, I.J. Fox, Treatment of cirrhosis and liver failure in rats by hepatocyte xenotransplantation, Gastroenterology 124 (2003) 422-431.

[6] R.A. Fisher, S.C. Strom, Human hepatocyte transplantation: worldwide results, Transplantation 82 (2006) 441-449.

[7] K.A. Soltys, A. Soto-Gutiérrez, M. Nagaya, K.M. Baskin, M. Deutsch, R. Ito, B.L. Shneider, R. Squires, J. Vockley, C. Guha, J. Roy-Chowdhury, S.C. Strom, J.L. Platt, I.J. Fox, Barriers to the successful treatment of liver disease by hepatocyte transplantation, J. Hepatol. 53 (2010)

769-774.

[8] A. Dhawan, J. Puppi, R.D. Hughes, R.R. Mitry, Human hepatocyte transplantation: current experience and future challenges, Nat. Rev. Gastroenterol. Hepatol. 7 (2010) 288-298.

[9] D.J. Anderson, A.D. Kirk, Primate models in organ transplantation, Cold Spring Harb. Perspect. Med. 3 (2013) a015503.

[10] K. Takahashi, K. Tanabe, M. Ohnuki, M. Narita, T. Ichisaka, K. Tomoda, S. Yamanaka, Induction of pluripotent stem cells from adult human fibroblasts by defined factors, Cell 131 (2007) 861-872.

[11] H. Liu, Y. Kim, S. Sharkis, L. Marchionni, Y.Y. Jang, In vivo liver regeneration potential of human induced pluripotent stem cells from diverse origins, Sci. Transl. Med. 3 (2011) 82ra39.

[12] Y. Shiba, T. Gomibuchi, T. Seto, Y. Wada, H. Ichimura, Y. Tanaka, T. Ogasawara, K. Okada, N. Shiba, K. Sakamoto, D. Ido, T. Shiina, M. Ohkura, J. Nakai, N. Uno, Y. Kazuki, M. Oshimura, I. Minami, U. Ikeda, Allogenic transplantation of iPS cell-derived cardiomyocytes regenerates primate hearts, Nature 538 (2016) 388-391.

[13] T. Kikuchi, A. Morizane, D. Doi, H. Magotani, H. Onoe, T. Hayashi, H. Mizuma, S. Takara, R. Takahashi, H. Inoue, S. Morita, M. Yamamoto, K. Okita, M. Nakagawa, M. Parmar, J. Takahashi, Human iPS cell-derived dopaminergic neurons function in a primate Parkinson's disease model, Nature 548 (2017) 592-596.

[14] R.B. Rutherford, J.K. Boitnott, J.S. Donohoo, E.G. Ohlsson, J. Sebor, G.D. Zuidema, The

production of biliary cirrhosis in Macaca mulatta monkeys, Arch. Surg. 100 (1970) 55-60.

[15] K. Ding, M.R. Liu, J. Li, K. Huang, Y. Liang, X. Shang, J. Chen, J. Mu, H. Liu, Establishment of a liver fibrosis model in cynomolgus monkeys, Exp. Toxicol. Pathol. 66 (2014) 257-261.

[16] T. Inoue, Y. Ishizaka, E. Sasaki, J. Lu, T. Mineshige, M. Yanase, E. Sasaki, M. Shimoda, Thioacetamide-induced hepatic fibrosis in the common marmoset, Exp. Anim. 67(3) (2018) 321-327.

[17] Y. Liu, C. Meyer, C. Xu, H. Weng, C. Hellerbrand, P. ten Dijke, S. Dooley, Animal models of chronic liver diseases, Am. J. Physiol. Gastrointest. Liver Physiol. 304 (2013) 449-468.

[18] M. Kotaka, T. Toyoda, K. Yasuda, Y. Kitano, C. Okada, A. Ohta, A. Watanabe, M. Uesugi, K. Osafune, Adrenergic receptor agonists induce the differentiation of pluripotent stem cell-derived hepatoblasts into hepatocyte-like cells, Sci. Rep. 7 (2017) 16734.

[19] J.J.H. Chong, X. Yang, C.W. Don, E. Minami, Y.W. Liu, J.J. Weyers, W.M. Mahoney Jr., B.V. Biber, S.M. Cook, N.J. Palpant, J.A. Gantz, J.A. Fugate, V. Muskheli, G.M. Gough, K.W. Vogel, C.A. Astley, C.E. Hotchkiss, A. Baldessari, L. Pabon, H. Reinecke, E.A. Gill, V. Nelson, H.P. Kiem, M.A. Laflamme, C.E. Murry, Human embryonic-stem-cell-derived cardiomyocytes regenerate non-human primate hearts, Nature 510 (2014) 273-277.

[20] Z.D. Goodman, Grading and staging system for inflammation and fibrosis in chronic liver diseases, J. Hepatol. 47 (2007) 598-607.

[21] N.H. Afdhal, D. Nunes, Evaluation of liver fibrosis: a concise review, Am. J. Gastroenterol. 99 (2004) 1160-1174.

[22] K.A. Soltys, K. Setoyama, E.N. Tafaleng, A. Soto Gutiérrez, J. Fong, K. Fukumitsu, T. Nishikawa, M. Nagaya, R. Sada, K. Harberman, R. Gramignoli, K. Dorko, V. Tahan, A. Dreyzin, K. Baskin, J.J. Crowley, M.A. Quader, M. Deutsch, C. Ashokkumar, B.L. Shneider, R.H. Squires, S. Ranganathan, M. Reyes-Mugica, S.F. Dobrowolski, G. Mazariegos, R. Elango, D.B. Stolz, S.C. Strom, G. Vockley, J. Roy-Chowdhury, M. Cascalho, C. Guha, R. Sindhi, J.L. Platt, I.J. Fox, Host conditioning and rejection monitoring in hepatocyte transplantation in humans, J. Hepatol. 66 (2017) 987-1000.

FIGURE LEGENDS

Fig. 1. Blood test results in macaques. (A) Schematic representation of the experimental design. TAA, thioacetamide; ceMRI, contrast-enhanced magnetic resonance imaging. (B-E) Serial changes in blood test results including serum ALT (B), serum iron (C), platelet count (D) and serum albumin (E). (F) Serial changes in ICG-R15 values. (G-I) Blood test results including prothrombin time (G), plasma ammonia (H) and serum total bilirubin (I). Control, fibrosis macaques #1-#3 before TAA administration and normal macaques #4-#6; 3M, 3 months; ALT, alanine aminotransferase; ICG-R15, indocyanine green retention rate at 15 minutes after intravenous injection. Data in the panels are presented as individual data points with means ±

s.d. *P < 0.05, **P < 0.01, ***P < 0.001, ****P < 0.0001, one-way ANOVA with Dunnett's correction for multiple comparisons.

Fig. 2. Sequential liver biopsies to assess liver fibrosis in macaques. (A) Azan staining ("Control" to "After 3M interval") and Masson's trichrome staining ("After euthanasia") of liver biopsy specimens of fibrosis macaques #1-#3. Scale bar, 200 μm. (B) Azan staining of liver biopsy specimens of normal macaques #4-#6. Portal, portal areas; Centrilobular, centrilobular areas. Scale bars, 100 μm. (C) Assessment of liver biopsy samples with the Ishak fibrosis score. (D) Serial changes in serum albumin concentrations during the interval stage. (E) Summary of serum hyaluronic acid concentrations. (F) Azan staining images of liver biopsy specimens of fibrosis macaque #3 after 6 and 12 months without TAA administration. Scale bars, 200 μm. (G) Serial changes in the Ishak fibrosis scores of fibrosis macaque #3. Data in (C) and (D) are presented as individual data points with means ± s.d. *P < 0.05, **P < 0.01, ***P < 0.001, ****P < 0.0001, one-way ANOVA with Sidak's correction (C) and Dunnett's correction (D) for multiple comparisons. M, month or months.

Fig. 3. Anatomical findings in macaques. (A) Gross appearance of the livers removed after euthanasia. The posterior segment of the macaque livers was lobulated. (B) The spleens of the macaques. (C) The size (length × width × height (cm^3)) of the spleens. (D) The veins draining

the descending colon. (E) Contrast-enhanced magnetic resonance imaging (ceMRI) images at the level of the gallbladder. Yellow arrows indicate the main trunk of the portal vein (PV). (F) The area of the PVs. Data in (C) and (F) are presented as individual data points with means. There are no data about macaque #1 in (C)-(F).

Fig. 4. Transplant of *ALB-GFP* reporter hiPSC-HLCs in the livers of fibrosis model macaques. (A) Schematic representation of the experimental design for the transplantation assay. TAA, thioacetamide; iv, intravenous injection; im, intramuscular injection. (B) Serial changes in whole blood concentrations of tacrolimus. (C, D) Phase-contrast (C) and fluorescent images (D) of an *ALB-GFP* reporter hiPSC-HLC aggregate. Scale bars, 100 μm. (E) A vessel catheter sheath was indwelled into a tributary of the inferior mesenteric vein. (F) Portal venography using the vessel catheter. RAP, right anterior portal branch; RPP, right posterior portal branch; LP, left portal vein. (G-I) Immunohistochemistry for GFP and human albumin (hALB) of the fibrotic livers of NHP models #1 (G), #2 (H) and #3 (I) on day 14 after the transplantation. Scale bars, 100 μm. (J, K) Immunohistochemistry for GFP of the normal livers of macaques #4 (J) and #5 (K) after euthanasia. Scale bars, 100 μm. (L-N) Immunohistochemistry for GFP followed by Masson's trichrome staining of the livers of NHP models #1 (L and M) and #2 (N) on day 14. Scale bars, 50 μm. Arrowheads indicate interlobular bile ducts in (G-N). Arrows indicate engrafted GFP-expressing cells in (L-N).

Table 1. Profiles of the six macaques used in this study.

Identifier	Sex	Age (y.o.)	Body weight (kg)		Stage (months)			hiPSC-HLC transplantation
			Before	After	1st	interval	2nd	
#1	Female	16	3.24	3.16	3	5	3	+
#2	Female	12	4.02	3.96	6	5	3	+
#3	Female	12	3.01	2.71	6	12	3	+
#4	Female	12	3.44	-	Normal liver			+
#5	Female	16	3.32	-	Normal liver			+
#6	Female	14	2.86	-	Normal liver			-

Because the supply of macaques was dependent on the situation of breeding, the six macaques were selected without randomization. Three macaques (#1, #2 and #3) underwent repeated TAA administration and the others (#4, #5 and #6) were used as normal controls. TAA, thioacetamide. hiPSC-HLC, human induced pluripotent stem cell-derived hepatocyte-like cell.

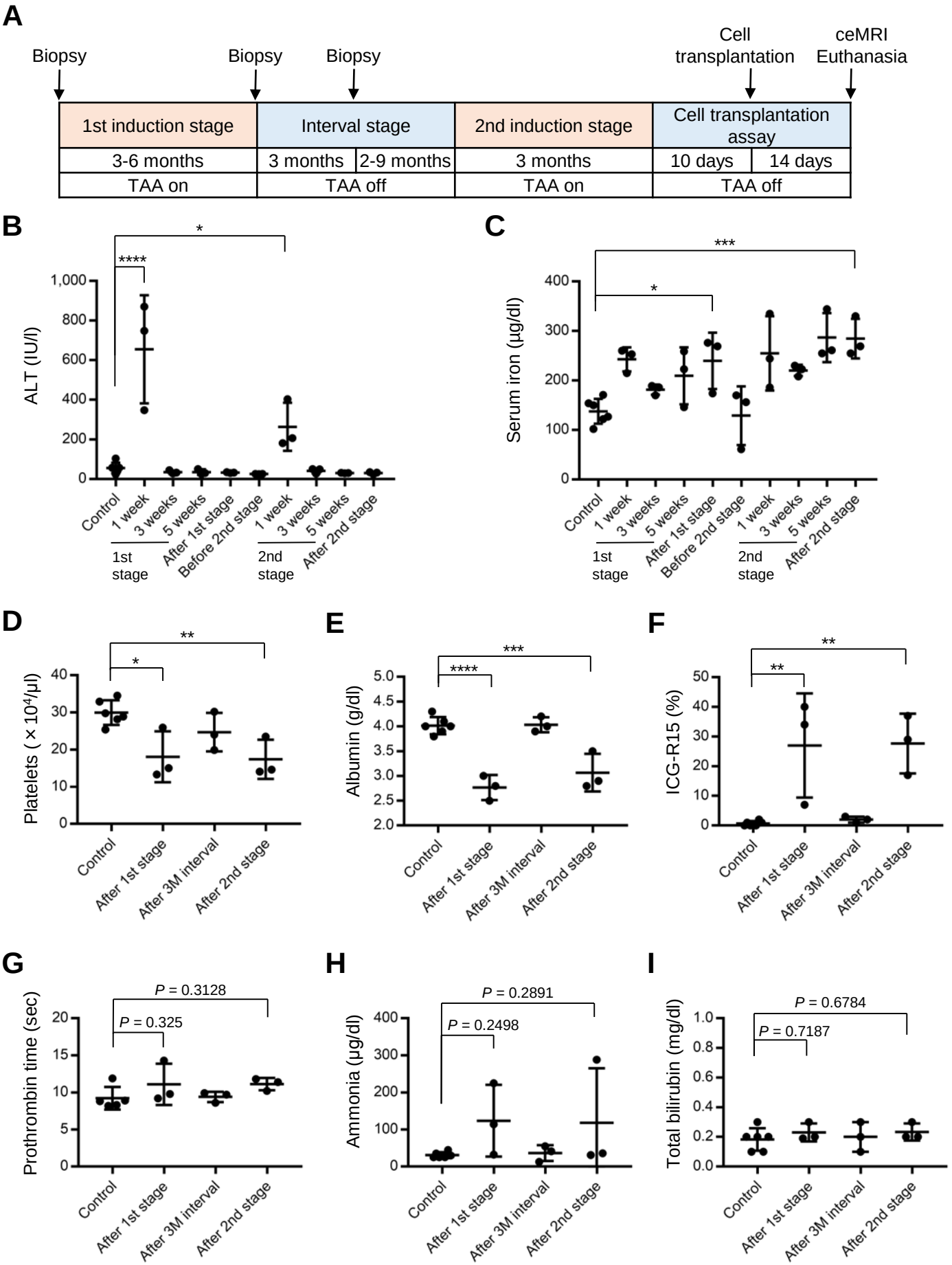
A
Biopsy
Biopsy
Biopsy
Cell transplantation
ceMRI Euthanasia
1st induction stage
Interval stage
2nd induction stage
Cell transplantation assay
3-6 months
3 months
2-9 months
3 months
10 days
14 days
TAA on
TAA off
TAA on
TAA off
B
ALT (IU/l)
Control
1 week
3 weeks
5 weeks
After 1st stage
Before 2nd stage
1 week
3 weeks
5 weeks
After 2nd stage
1st stage
2nd stage
C
Serum iron (μg/dl)
D
Platelets (×10⁴/μl)
E
Albumin (g/dl)
F
ICG-R15 (%)
G
Prothrombin time (sec)
P = 0.3128
P = 0.325
H
Ammonia (μg/dl)
P = 0.2891
P = 0.2498
I
Total bilirubin (mg/dl)
P = 0.6784
P = 0.7187
After 1st stage
After 3M interval
After 2nd stage

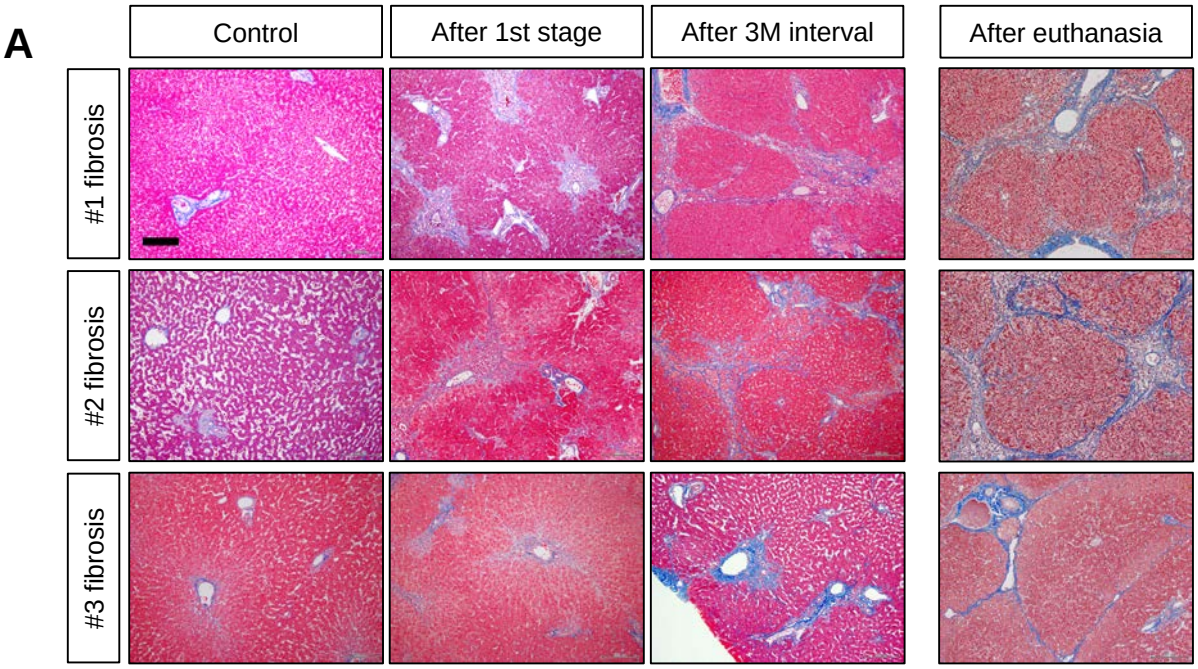

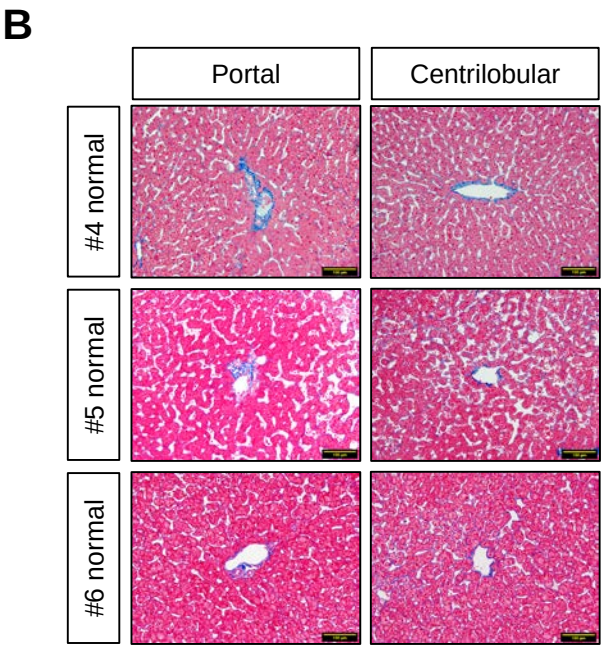

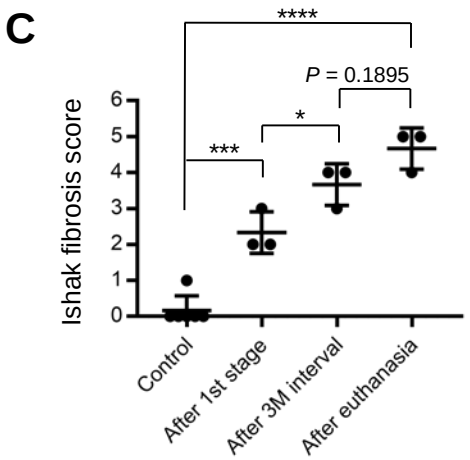

E

	#1 fibrosis	#2 fibrosis	#3 fibrosis
Control	61.7	21.1	54.1
After 1st stage	229.7	3552.3	1791.1
After 1M interval	88.6	149	67.1
After 2M interval	105.8	53.4	71.8
After 3M interval	84.8	71.1	58.3

Serum hyaluronic acid (ng/ml)

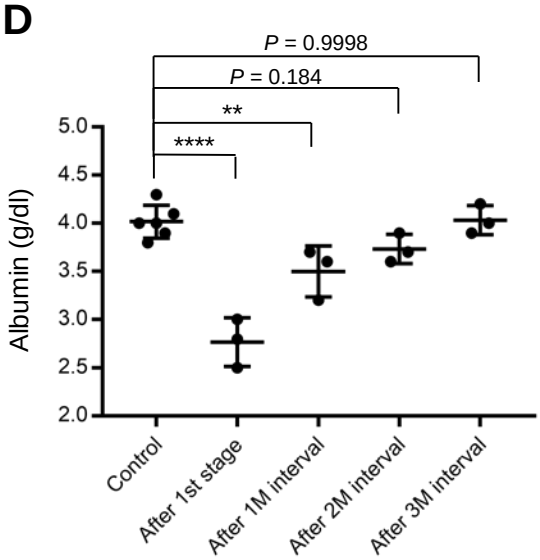

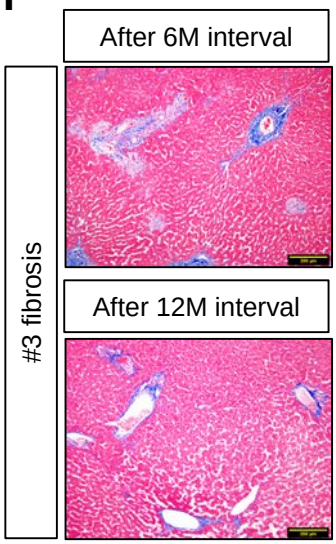

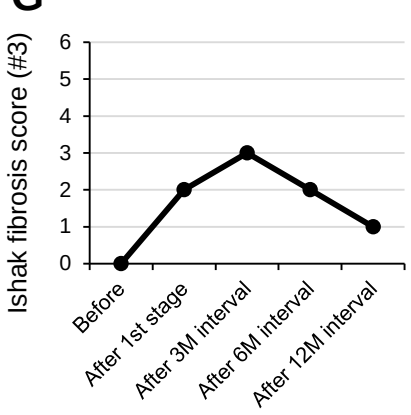

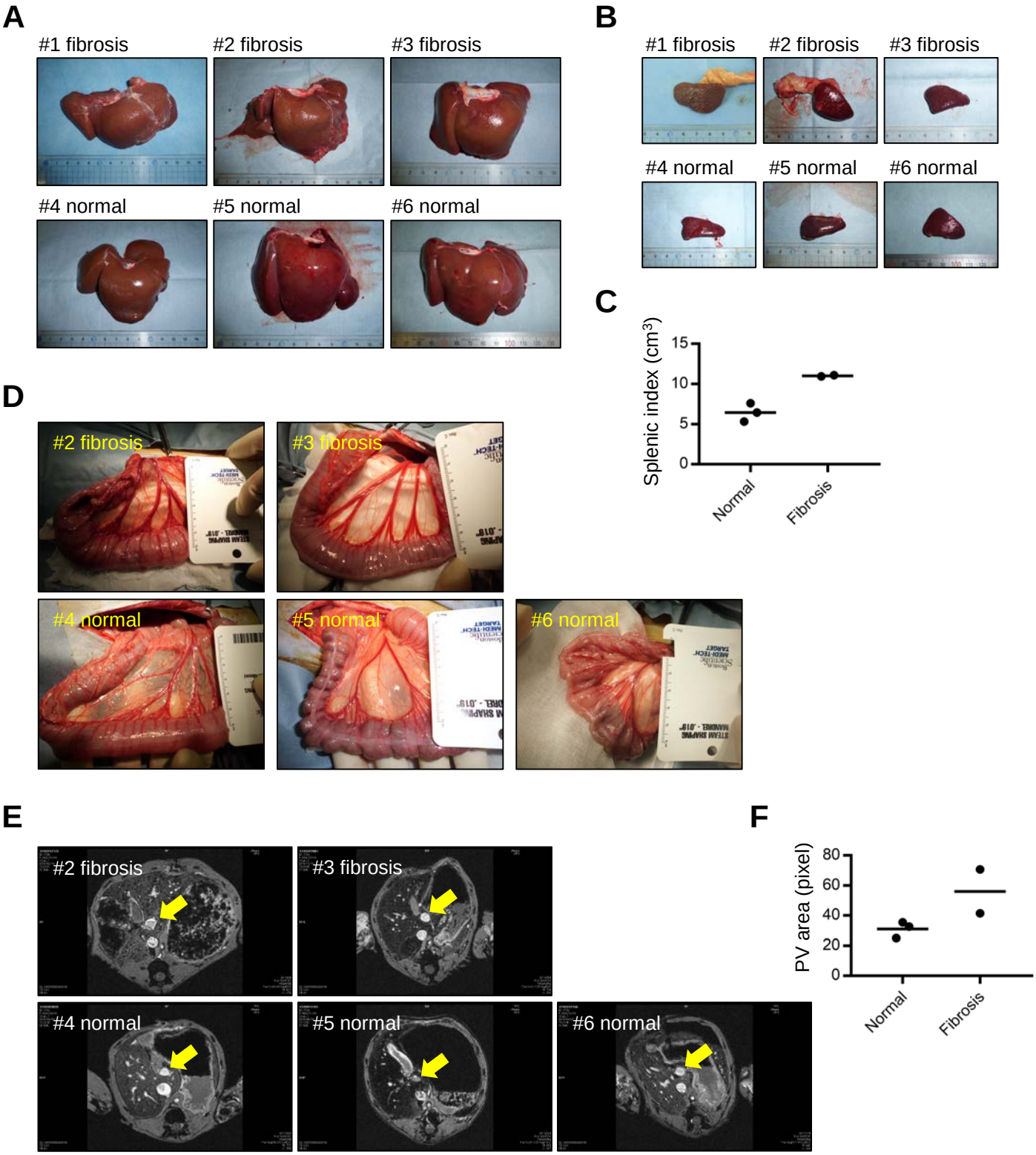
A
#1 fibrosis
#2 fibrosis
#3 fibrosis
#4 normal
#5 normal
#6 normal
B
#1 fibrosis
#2 fibrosis
#3 fibrosis
#4 normal
#5 normal
#6 normal
C
Splenic index (cm3)
15
10
5
0
Normal
Fibrosis
D
#2 fibrosis
#3 fibrosis
#4 normal
#5 normal
#6 normal
E
#2 fibrosis
#3 fibrosis
#4 normal
#5 normal
#6 normal
F
PV area (pixel)
80
60
40
20
0
Normal
Fibrosis

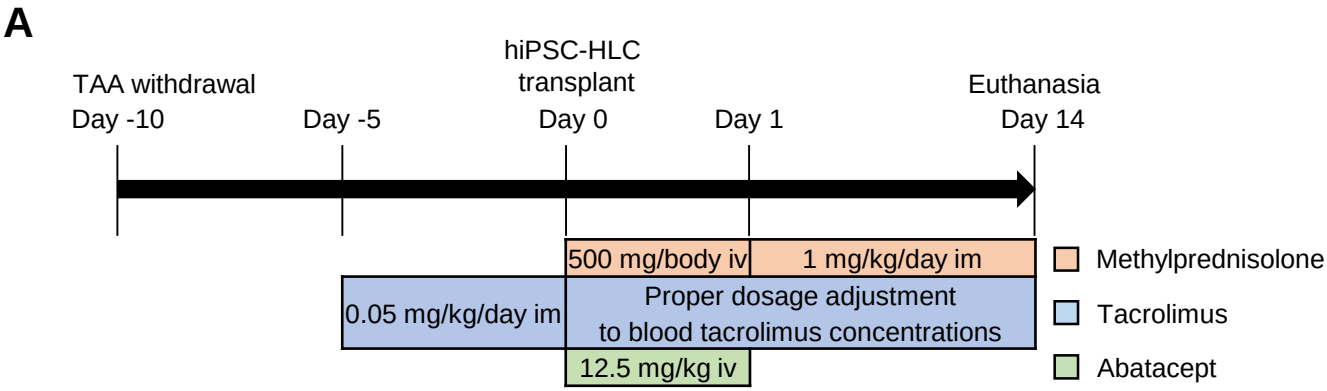
A
TAA withdrawal
Day -10
Day -5
hiPSC-HLC
transplant
Day 0
Day 1
Euthanasia
Day 14
500 mg/body iv
1 mg/kg/day im
0.05 mg/kg/day im
Proper dosage adjustment
to blood tacrolimus concentrations
12.5 mg/kg iv
Methylprednisolone
Tacrolimus
Abatacept

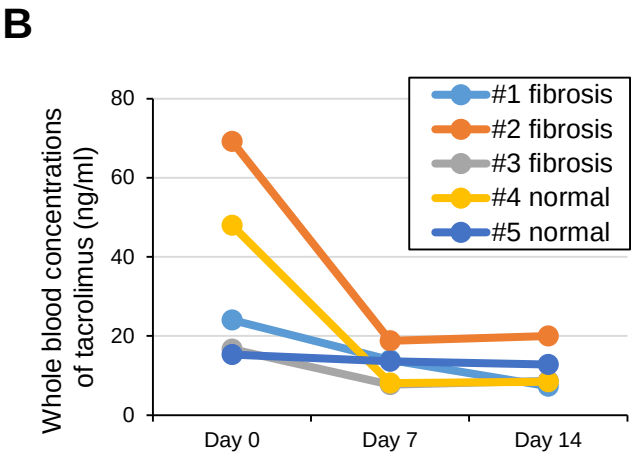
B
Whole blood concentrations
of tacrolimus (ng/ml)
80
60
40
20
0
Day 0
Day 7
Day 14
#1 fibrosis
#2 fibrosis
#3 fibrosis
#4 normal
#5 normal

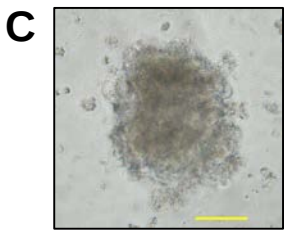
C

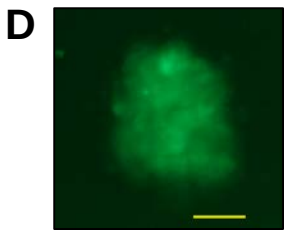
D

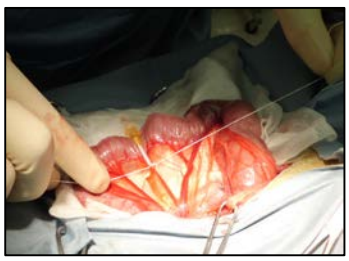
E

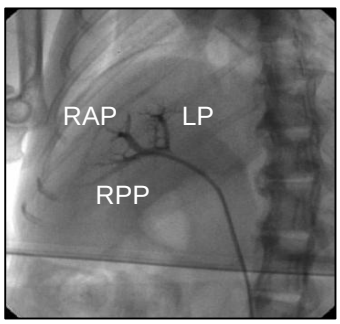
F
RAP
LP
RPP

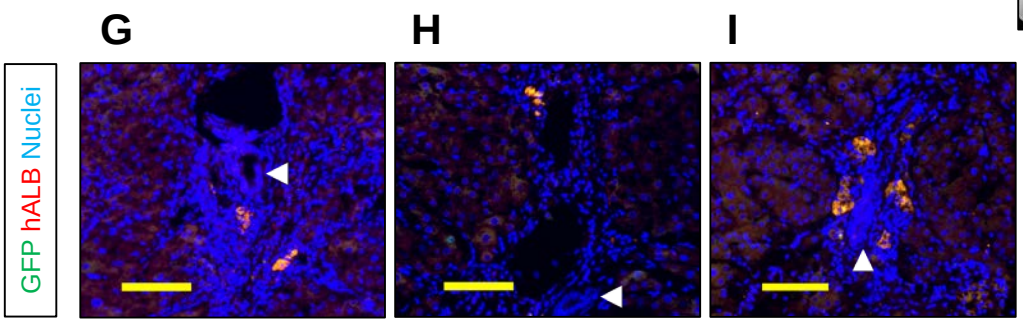
G
H
I
GFP hALB Nuclei

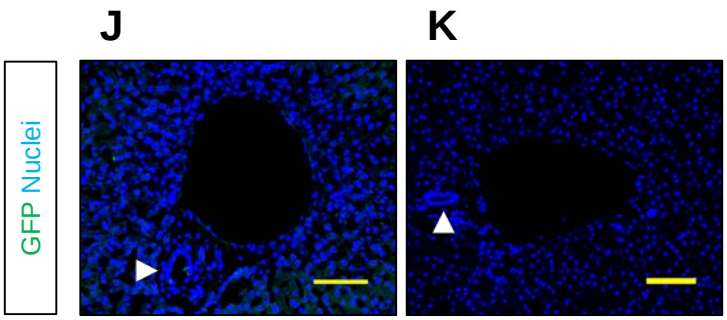
J
K
GFP Nuclei

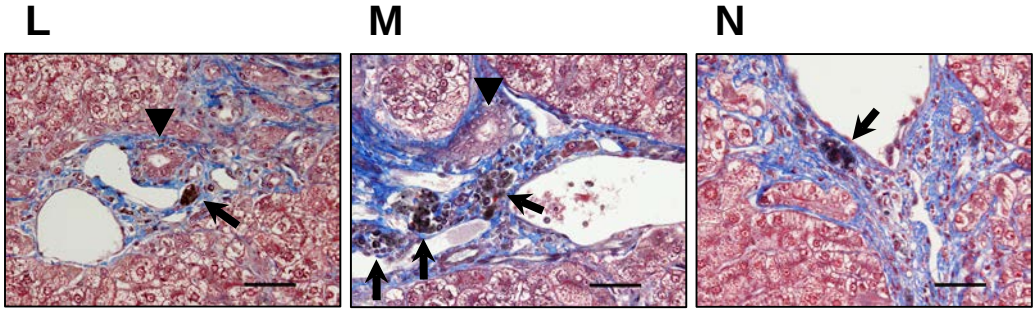
L
M
N